



HAL
open science

Degradation of diatom carbohydrates: A case study with N- and Si-stressed *Thalassiosira weissflogii*

Maxime Suroy, Christos Panagiotopoulos, Julia Boutorh, M. Goutx, Brivaëla
Moriceau

► **To cite this version:**

Maxime Suroy, Christos Panagiotopoulos, Julia Boutorh, M. Goutx, Brivaëla Moriceau. Degradation of diatom carbohydrates: A case study with N- and Si-stressed *Thalassiosira weissflogii*. *Journal of Experimental Marine Biology and Ecology*, 2015, 470, pp.1-11. 10.1016/j.jembe.2015.04.018 . hal-03622281v2

HAL Id: hal-03622281

<https://hal.science/hal-03622281v2>

Submitted on 13 Dec 2023

HAL is a multi-disciplinary open access archive for the deposit and dissemination of scientific research documents, whether they are published or not. The documents may come from teaching and research institutions in France or abroad, or from public or private research centers.

L'archive ouverte pluridisciplinaire **HAL**, est destinée au dépôt et à la diffusion de documents scientifiques de niveau recherche, publiés ou non, émanant des établissements d'enseignement et de recherche français ou étrangers, des laboratoires publics ou privés.

Degradation of diatom carbohydrates: A case study with N- and Si-stressed *Thalassiosira weissflogii*

Maxime Suroy^a, Christos Panagiotopoulos^{a,*}, Julia Boutorh^b, Madeleine Goutx^a, Brivaëla Moriceau^b

^a Aix Marseille Université, CNRS/INSU, Université de Toulon, IRD, Mediterranean Institute of Oceanography (MIO), UM 110, 13288, Marseille, France

^b Université de Brest, Institut Universitaire Européen de la Mer (IUEM), CNRS, Laboratoire des Sciences de l'Environnement Marin, UMR 6539 CNRS/UBO/IFREMER/IRD, 29280 Plouzané, France

ARTICLE INFO

Article history:

Received 22 September 2014

Received in revised form 19 April 2015

Accepted 20 April 2015

Available online xxxx

Keywords:

Thalassiosira weissflogii

Biodegradation experiment

Carbohydrates

N- and Si-limitation

Degradation rate constants

ABSTRACT

Diatoms are a key phytoplanktonic group that affects the carbon cycle in the ocean. Although the effect of nutrient limitation on the primary productivity of diatoms is well-studied, the effect of such a limitation on the organic matter quality of diatoms and their vertical transport through the water column remains unclear. In this study, the diatom *Thalassiosira weissflogii* (TW) was grown under two different nutrient conditions, 'N-stress' and 'Si-stress', and was compared against healthy TW cells (Nutrient-replete). Biodegradation experiments of TW were performed for all of the above conditions, and the particulate fraction was monitored over time (~one month) in terms of the organic carbon (POC), nitrogen (PON), and sugars (PCHO), including prokaryotic counting. Using these results, we estimated the degradation rate constants for POC, PON, PCHO, and the individual carbohydrate monomers (monosaccharides) for the TW cells. Our results indicated that the N- and Si-limitations increase the organic carbon content of the TW cells with a concomitant decrease in the silicon content (bSiO₂), suggesting a modification of the TW cells. The PCHO content increased by a factor of 2.6 and 3.8 in the N-stress and Si-stress cells, respectively. At the beginning of the experiment (T₀), the N-stress and Si-stress cells were characterized by higher amounts of glucose (5–32 mol%) and xylose (13–19 mol%), compared with the Nutrient-replete cells, which were dominated by ribose (~22 mol%), indicating differences in the physiological status of the TW cells and/or in the synthesis of storage/structural polysaccharides. The first order degradation rate constants (k₁) for the POC were similar in all of the experiments (k₁ = 0.096–0.113 d⁻¹), which was not the case for the PON in which the highest values (by a factor of ~2.5) were observed for the nutrient-replete experiment. This result indicates a different behavior in the utilization and/or accessibility to prokaryotes of carbon and nitrogen during the biodegradation experiment. Moreover, ribose, glucose, and galactose exhibited the highest degradation rate constants in all of the experiments, which further reflects the differences in their initial macromolecular origin (e.g., storage vs structural carbohydrates) and highlights the changes in the organic matter quality during growth under nutrient-limited conditions and degradation. These results suggest that the 'nutrient-stress' diatoms may affect the export of carbon (particularly carbohydrates) relative to nitrogen in the ocean interior compared with the diatoms grown under optimal conditions.

1. Introduction

Diatoms are a key phytoplanktonic group responsible for nearly 25 to 35% of the total primary production in oceans (Aumont et al., 2003; Nelson et al., 1995; Uitz et al., 2010). Moreover, diatoms are important contributors to organic carbon export because they are often associated with the formation of large aggregates made of fresh material or phytodetritus that rapidly sink to the ocean interior, with sinking velocities averaging ~100 m d⁻¹ (Goutx et al., 2007; Martin et al., 2011; Sarthou et al., 2005). Finally, diatoms form most of the sedimentation fluxes along with coccolithophores (Engel et al., 2009) and large fecal pellets (Thornton, 2002; Turner, 2002); therefore, they considerably

influence the functioning of the biological carbon pump (Buesseler, 1998; Volk and Hoffert, 1985).

The efficiency of the diatoms to export organic carbon to the ocean interior depends not only on their productivity, but also on the balance between the sinking velocity of the particles and their degradation rates, both of which are controlled by biotic and abiotic parameters. These parameters include aggregation/disaggregation rates of the particles (Logan et al., 1995), particle size/density (De La Rocha and Passow, 2007 and references therein), the prokaryotic community attached to the particles (Legendre and Rivkin, 2002), temperature (Bidle et al., 2002; Iversen and Ploug, 2013), pressure (Tamburini et al., 2006), and the presence of minerals (Engel et al., 2009; Honda and Watanabe, 2010; Moriceau et al., 2009).

Nutrient limitations are known to affect the production of diatoms; however, significantly less is known about their effect on diatom export.

* Corresponding author.

E-mail address: christos.panagiotopoulos@mio.osupytheas.fr (C. Panagiotopoulos).

Nitrogen and silicon are the two major nutrients limiting diatom productivity in the open ocean (Moore et al., 2002). Nitrogen is considered to be the main element controlling primary marine production in the ocean, whereas silicon is only required for silicified species, such as diatoms (Falkowski, 1997). Nutrient availability acts on the sinking velocities of a diatom by inducing biochemical composition changes that can modify the organic matter (OM) quality and the cell buoyancy (Lynn et al., 2000; Richardson and Cullen, 1995; Shifrin and Chisholm, 1981). Nitrogen and silicon limitation generally results in a decrease in the growth rate of diatoms (Claquin et al., 2002; Martin-Jézéquel et al., 2000), the nutrient uptake (De La Rocha et al., 2010), and a decrease in the free amino acid and protein content (Martin-Jézéquel et al., 2000; Palmucci et al., 2011). The modulation of the cell cycle involving these limitations also affects the frustule silicification (Claquin et al., 2002; Martin-Jézéquel et al., 2000). Generally, frustules of nitrogen-limited diatoms are thicker than those of silicon-limited diatoms due to a longer cell cycle, which further indicates a decoupling between the silicon and nitrogen metabolisms (Claquin et al., 2002; Hildebrand, 2002).

Although the effect of nutrient limitation on the biochemical composition of diatoms cannot be generalized because of their different specific responses (Palmucci et al., 2011; Shifrin and Chisholm, 1981), generally the decrease in growth rate results in a decrease in the protein synthesis, which is compensated by an increase in storage compounds (e.g., carbohydrates). For example, nitrogen starvation results in an accumulation of carbohydrates and a decrease in lipids (Shifrin and Chisholm, 1981; Suroy et al., 2014) in TW, an important diatom species that dominates phytoplankton blooms after a nutrient input in certain oceanic areas (Smetacek, 1985; Sorhannus et al., 2010). Although a significant number of studies has focused on the degradation of particles and/or diatoms by following their bulk individual components (e.g., proteins, carbohydrates, lipids, etc.; Harvey et al., 1995; Panagiotopoulos et al., 2002), very few data currently exist at the molecular level regarding the above compound classes (Goutx et al., 2007; Harvey and Macko, 1997) and especially those of carbohydrates.

To the best of our knowledge only the dynamics of amino acids have been explored during the decomposition of calcifying and non-calcifying *Emiliania huxleyi* cultures (Engel et al., 2009), whereas very little information exists on carbohydrates. Although carbohydrates are less abundant in diatoms (~5–10% of their total dry weight; Brown et al., 1997) compared with amino acids, they are among the most abundant compounds in particulate (5–15%; Hernes et al., 1996; Panagiotopoulos and Sempéré, 2005a) and dissolved organic matter (2–10%; Panagiotopoulos and Sempéré, 2005b and references therein).

The present study aims to explore the carbohydrate changes at the molecular level of the diatom cells under variable environmental growth conditions and particularly assess the effect of nutrient stress during biotic degradation. We used *Thalassiosira weissflogii* (TW) as a model diatom and we tested the effect of two different nutrient stress conditions (nitrogen and silicon starvations) on its carbohydrate composition. Degradation of nutrient-stress algae was monitored over time (30 days), and the degradation rate constants of the individual monosaccharides were estimated. The results are compared and discussed along with the bulk degradation features of the particulate organic carbon and nitrogen.

2. Materials and methods

2.1. Experimental design

The experimental protocol consisted of the production of TW cells which were grown in three different conditions namely: 'Nutrient-replete', 'N-stress', and 'Si-stress' followed by a degradation experiment (Fig. 1). As such, the above TW cells were incubated in the darkness with the presence of a natural prokaryote community.

2.1.1. "Nutrient-replete" and "Nutrient-stress" cultures

TW was grown in Conway medium (Walne, 1966) in a large volume container culture at the Argenton Ifremer station at 20 °C under a 12 h:12 h light:dark cycle and an irradiance of 241 $\mu\text{mol photons m}^{-2} \text{s}^{-1}$. A volume (10 L) of culture at a cell concentration of $4.0 \pm 0.26 \times 10^8 \text{ cell L}^{-1}$ was centrifuged and the produced pellet was stored in the freezer ($-20 \text{ }^\circ\text{C}$) for one week. This material corresponded to the "Nutrient-replete" cells. An additional volume of 20 L was equally divided into two aliquots (Table 1). The cells were centrifuged, rinsed with artificial seawater and resuspended in two container cultures filled with f/2 medium, NO_3^- and H_4SiO_4 free, for the N-stress and Si-stress experiments, respectively. Because of laboratory logistical constraints, "Nutrient-replete" and "Nutrient-stress" cells were produced in different growth media (Conway medium vs f/2 medium). Previous studies showed little difference in the diatom growth between f/2 and Conway media (Lahanan et al., 2013); therefore we may confidently consider that the growth of TW in the Conway medium is representative of our "Nutrient-replete" cells and comparable to the "Nutrient-stress" cultures.

The 'N-stress' and 'Si-stress' diatom container cultures were placed at 18 °C in a growth chamber under a 12 h:12 h light:dark cycle at an irradiance of 158 $\mu\text{mol photons m}^{-2} \text{s}^{-1}$ for one week. The silicic acid (dSi), pH, nitrates, and phosphates were measured over time to control the growth conditions of the cells (Boutorh et al. *comm. pers.*). For the 'N-stress' culture, the nitrate concentrations were below the detection limit immediately after the beginning of the starvation procedure, indicating an efficient starvation. Similarly, during the Si-starvation experiment, the dSi concentrations ranged from 0 to 3.4 μM . The low dSi concentrations were likely due to the dissolution of a certain amount of dead cells, but the diatom still underwent Si-starvation (Sarhou et al., 2005). Moreover, during the Si-starvation, the pH concentrations increased over time and reached values >9.3 after day 6, indicating a C-limitation. This pattern was not observed in the 'N-stress' culture in which the dSi concentrations decreased over time to reach values <3.0 μM at day 6, indicating a late Si-limitation. Similar to the above procedure, after one week of growth, the diatoms were concentrated by centrifugation and killed by freezing at $-20 \text{ }^\circ\text{C}$. This was confirmed by flow cytometry which showed that about 98% of the TW were killed at $-20 \text{ }^\circ\text{C}$, while the cell integrity was not disrupted (Soler, 2010).

2.1.2. Degradation experiments

The TW cells ('Nutrient-replete', 'N-stress', and 'Si-stress') were resuspended in 10 L degradation batches, filled with 0.8 μm filtered natural seawater sampled at a 10 m depth in the Bay of Brest (4° 33' 07.19 W, 48° 21' 32.13 N) in October 2011 (Fig. 1). The physical and chemical hydrological characteristics of the area are provided at the following link: <http://somlit.epoc.u-bordeaux1.fr/fr/>. The seawater was filtered on 0.8- μm polycarbonate membrane (Millipore) to remove the phyto- and zooplanktonic organisms while maintaining most of the natural prokaryotic community (Duhamel et al., 2007). Epifluorescence microscopy analysis of the 0.8 μm filtrate revealed the presence of the autochthonous prokaryotic community and very few picoeucaryotes cells (results not shown) which agrees with previous studies (Duhamel et al., 2007).

The degradation batches were placed on an orbital shaker table at 16 °C in the dark, and punched caps were used to ensure gas exchange. The batches were sampled for the biochemical parameters (POC, PON, and PCHO), including the total count of the heterotrophic prokaryotes over 30 days. Prior to each sampling, the batches were vigorously shaken to ensure homogeneity. At the end of the degradation experiment, more than the half of the initial volume remained (~6 L) in the bottle to reduce the experimental errors related to the sample amounts. The number of replicates for each parameter (POC, PON, and PCHO) is indicated in the figure legends.

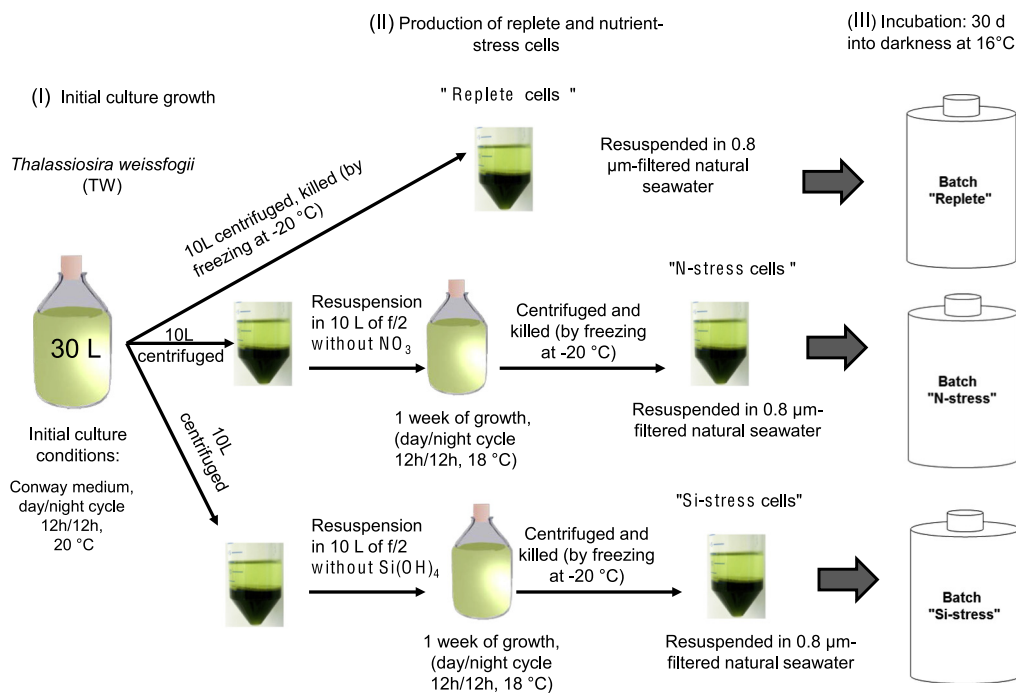


Fig. 1. Schematic presentation of the experimental design and sampling of TW cells.

2.2. POC and PON measurements

Each day, 10 mL of culture was filtered on pre-combusted GF/F filters (5 h, 450 °C) for the POC and PON concentration measurements. The filters were dried overnight in an oven at 50 °C. The POC and PON levels were measured on the same filter using a Carlo Erba NA 2100 CN analyzer coupled to a Finnigan Delta S mass spectrometer (Nieuwenhuize et al., 1994). The detection limit was 5 and 1 µg for POC and PON, respectively, with a standard error of 2–3%.

2.3. Prokaryotic carbon and nitrogen concentration

The prokaryotic cells were counted over time at each day-point of the degradation experiment to evaluate their growth. Total and free prokaryotes were counted before and after filtration on a 0.3 µm pore size filter, respectively, in 10 mL samples stained with DAPI (4',6-diamidino-2-phenylindole). The number of attached prokaryotes was calculated by subtracting the number of free-prokaryotes in the 0.3 µm filtrate from the total prokaryote number. It is important to note that to detach prokaryotes from diatomaceous particles a sequestering/deflocculating agent is added to the total sample (Velji and Albright, 1986). Then the sample was centrifuged at low speed to remove large particles without causing sedimentation of bacteria.

The amount of prokaryotic carbon during the degradation experiment was calculated using the conversion factors (20 and 50×10^{-15} mol C cell⁻¹ for the free and attached prokaryotes, respectively) proposed by Turley and Mackie (1994). Similarly, the amount of prokaryotic nitrogen was calculated using the N/C ratio of 0.28 proposed by Fagerbakke et al. (1996). Thus, the organic carbon from the diatoms was defined as $POC - POC_{\text{attached prokaryotic-C}}$ and the organic nitrogen from the diatoms was defined as $PON - PON_{\text{attached prokaryotic-N}}$.

2.4. Particulate carbohydrates (PCHO) analysis

2.4.1. PCHO extraction and isolation

Similar to the POC and PON measurements, 10 mL of culture was filtered on GF/F filters for the PCHO analysis. The filters were cut with

clean scissors and transferred to 15 mL glass tubes with Teflon-lined screw caps to which 6 mL of 1.2 M H₂SO₄ was added. The samples were bubbled with N₂ and hydrolyzed in a sand bath for 3 h at 100 °C (Cowie and Hedges, 1984; Panagiotopoulos and Wurl, 2009). The hydrolysis was stopped by placing the tubes in an ice bath for 5–10 min. The samples were neutralized with pre-combusted CaCO₃ (450 °C for 5 h) and centrifuged 3–4 times at 4000 rpm for 5 min. The supernatant was filtered through pre-combusted quartz wool (450 °C for 5 h) and pipetted into scintillation vials. The vials were maintained at 4 °C until the time of analysis (this time never exceeded 24 h).

2.4.2. Liquid chromatography

A Dionex ICS-3000 anion exchange chromatograph fitted with a pulsed amperometric detector (HPAEC-PAD) was used for all PCHO analyses. The separation of the PCHO was performed on a Dionex CarboPac PA-1 analytical column and a Dionex CarboPac PA-1 guard column. An amino trap was placed before the guard column to retain the amino acids and similar compounds, which may interfere with the PCHO analysis. The analytical column, the guard column, and the amino trap were placed into a thermal compartment set at 17 °C (Panagiotopoulos et al., 2012). Sugars were detected by an electrochemical detector (ED40-Dionex) set in the pulsed amperometric mode (standard quadruple potential).

Ten individual monosaccharides were detected in the hydrolysates of the particulate organic material, including deoxysugars (fucose, and rhamnose), pentoses (arabinose, ribose, and xylose), one amino sugar (glucosamine), hexoses (galactose, glucose, and mannose), and one acidic sugar (galacturonic acid). The neutral and amino sugars were separated with an isocratic 19 mM NaOH elution at 17 °C (eluent A: 20 mM NaOH; eluent B: Milli Q water). Galacturonic acid was detected in a separate analysis using a gradient of two mobile phases (eluent C: 1 M NaOH; eluent D: 0.5 M CH₃COONa) according to Panagiotopoulos et al. (2012). The flow rate was set at 0.7 ml min⁻¹ for the neutral and acidic sugar analyses. The data acquisition and processing were performed using the Dionex software Chromeleon®. The analytic errors calculated by the coefficients of variation of the repeated injections of a standard solution of 50 nM/sugar were 5–10% and 0.9–2.0% (n = 6) for the peak area and the retention time, respectively.

Table 1
Initial parameters measured in each batch at the beginning of the experiment. The prokaryotic inoculum concentrations were estimated before the addition of the diatom cells.

Growth conditions	Batch volume (L)	[Diatom cells] (cell L^{-1})	Cellular volume ^a (μm^3)	[POC] ^b /[diatom cell] (pmol cell^{-1})	[PON] ^b /[diatom cell] (pmol cell^{-1})	[Inoculum] (cell L^{-1})	[SiO_2]/[diatom cell] (pmol cell^{-1})
Nutrient-replete	10	1.80×10^8	1488 ± 117	8.14	1.17	5.00×10^9	1.90
N-stress	10	3.02×10^8	1154 ± 137	14.39	0.73	2.55×10^9	0.89
Si-stress	10	2.11×10^8	1364 ± 150	17.41	1.51	5.39×10^9	0.86

^a Cellular volumes were calculated at the end of the starvation experiment.

^b POC and PON values were corrected from the carbon and nitrogen contributions of the attached prokaryotes, respectively (see Section 2.3).

2.5. Statistical analysis and kinetic parameters estimation

To compare the contributions of the monosaccharides to the diatom composition in the three treatments at day 1 (triplicates), a *Kruskal–Wallis* test was performed using the R freeware (R Core Team, 2012). Our null hypothesis was that there is no difference in the monosaccharide contributions between the batches. We fixed the significance level at 5%. For each comparison showing a significant difference, a multiple comparison between the treatments was used to determine the batch that was different (Giraudoux, 2012).

The degradation rate constants of the bulk parameters (POC and PON) were calculated assuming two pools of organic matter (Moriceau et al., 2009). These two pools can be successively or simultaneously degraded and a OD model can be applied to estimate the different degradation rate constants.

Statistically, the POC and DON data are best fitted with the model using two successive exponential decay equations, as follows:

$$C(t) = C_0 \exp(-k_1 t), \quad 0 < t < t_s \quad (1)$$

$$C(t) = C(t_s) \exp(-k_2(t - t_s)), \quad t > t_s \quad (2)$$

$C(t)$ represents the concentration at day t , C_0 is the initial concentration, t is the time in days, k_1 and k_2 are the two degradation rate constants, and t_s is the substitution time at which the degradation rate constant shifts from k_1 to k_2 .

Total carbohydrate (PCHO) and individual monosaccharide concentration values were best fitted into the model using only one exponential decay equation, which is in agreement with previous studies (Giroldo et al., 2003; Goutx et al., 2007; Moriceau et al., 2009), according to the following equation:

$$C(t) = C_0 \exp(-kt) \quad (3)$$

The kinetic parameters for the monosaccharide degradation were calculated with a non-linear least square model using the *nls* function in the R freeware (R Core Team, 2012). Finally, the *t*-test was used to test the null hypothesis on our measured parameters (POC, PON, and PCHO).

3. Results

3.1. Initial observations

At the beginning of the biodegradation experiment, diatom cell concentrations were $1.80 \times 10^8 \text{ cell L}^{-1}$ in the 'Nutrient-replete' batch, $2.11 \times 10^8 \text{ cell L}^{-1}$ in the 'Si-stress' batch, and $3.02 \times 10^8 \text{ cells L}^{-1}$ in the 'N-stress' batch (Table 1). The N- and Si-stress growth conditions induced an increase in the carbon content per cell compared with the 'Nutrient-replete' diatoms (8.14, 14.39, and 17.41 pmol cell^{-1} in the 'Nutrient-replete', 'N-stress', and 'Si-stress' batches, respectively) (Table 1).

The 'Si-stress' and 'N-stress' diatoms had a lower cellular volume than the 'Nutrient-replete' diatoms. The 'N-stress' and the 'Si-stress' cells

contained approximately two times the amount of organic carbon than the 'Nutrient-replete' cells (Table 1), which was even more pronounced when estimated on a per volume liter basis (12.47, 12.76, and 5.47 pmol cell^{-1} , respectively). The organic nitrogen content did not follow the organic carbon patterns and was lower in the 'N-stress' cells (0.73 pmol cell^{-1}) than in the 'Nutrient-replete' (1.17 pmol cell^{-1}) and 'Si-stress' cells (1.51 pmol cell^{-1}) (Table 1). Similar to previous results, these differences were observed when estimated on a per volume basis.

The concentration of the prokaryotic inoculums was of the same order of magnitude in all of the batches at T_0 indicating the same bacterial number ($\sim 10^9 \text{ cell L}^{-1}$) at the beginning of the experiments (Table 1). The prokaryotic concentrations in the three batches showed the same global trend over time, reaching a maximum at day 3 followed by a decrease until reached a steady state (Fig. 2). It is worth noting that prokaryotic concentrations reached this steady state ($\sim 40 \times 10^9 \text{ cell L}^{-1}$) in the 'Nutrient-replete' batch much earlier (at day 6) than in the 'N-stress' and 'Si-stress' batches (after ~ 15 days) (Fig. 2). This difference may be explained by the initially higher concentrations of the POC in the N- and Si-stressed cell batches (Table 1).

Our results showed an increase in the POC concentrations (approximately 7–30% of the initial POC) which was observed between T_0 and T_1 in all three batches (Fig. 2). Then POC concentrations decreased over time till the end of the experiment. The growth of the attached prokaryotes at day 1 (Fig. 2) explained only 7.5%, 0.9% and 1.2% of the increase of the POC at day 1 in the 'Nutrient-replete', 'N-stress', and 'Si-stress' experiments, respectively. This result further indicates that the increase in POC at day 1 is most likely related to a combination of biotic and abiotic processes at the beginning of the degradation experiments (e.g., agglomeration of POC due to heterogeneity, prokaryotes growth, a low TEP production by bacteria) including analytical error (Fig. 3). The increase in the POC at day 1 may also be related to the absorption/

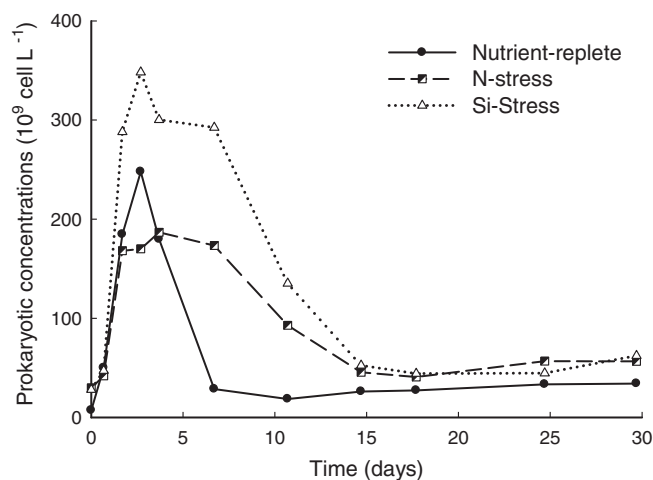


Fig. 2. Evolution of the prokaryotic concentrations over time in the 'Nutrient-replete', 'N-stress', and 'Si-stress' batches during the biodegradation experiments. The prokaryotic concentrations correspond to the sum of the free and attached prokaryotes. $N = 1$ at each sampling point.

desorption phenomena of the suspended particles on the bottle wall during biodegradation. These observations (increase of POC at day 1) have been previously reported in particle or diatom biodegradation experiments (Engel et al., 2009; Panagiotopoulos et al., 2002).

After day 1, POC decreased over time while we observed an increase in the bacterial numbers, which typically reflects the decomposition pattern of TW-POC. For all of these reasons mentioned above, we have chosen to consider the data at T_1 as the beginning of the degradation.

Similar to the POC levels, the PON concentrations also showed an increase at day 1 in all of the batches (+70.1, +58.4 and +55.6% of the initial PON concentrations in the 'Nutrient-replete', 'N-stress' and 'Si-stress' batches, respectively). Using conversion factors to estimate the organic nitrogen contribution from the prokaryotes (see the [Materials and methods](#) section), the prokaryotic nitrogen accounted for 13, 10 and 8% of the total PON at day 1 in the 'Nutrient-replete', 'N-stress' and 'Si-stress' batches, respectively.

The C/N ratio was equal to 7.0 at the beginning of the degradation experiment in the 'Nutrient-replete' batch, which is in the range of the previously reported values for TW (C/N = 5–9; Brzezinski, 1985; De La Rocha et al., 2010). This ratio was strongly influenced by the nutrient stress, with an increase of up to 11.5 in the 'Si-stress' cells and 19.7 in the 'N-stress' cells.

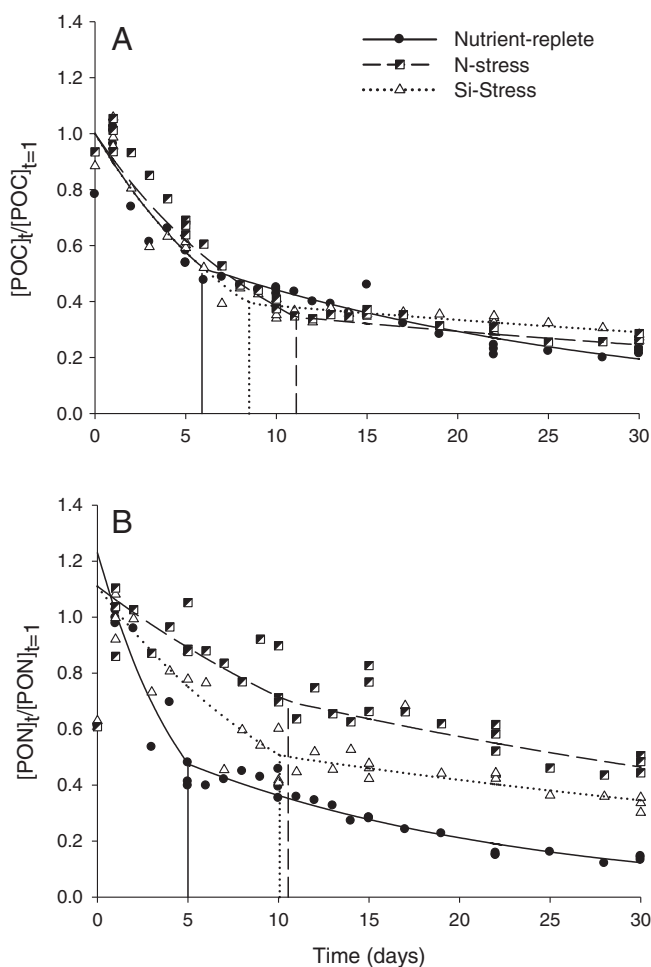


Fig. 3. Time course responses of the (A) POC and (B) PON relative concentrations of TW in the 'Nutrient-replete', 'N-stress', and 'Si-stress' batches. The relative concentrations were calculated by dividing the concentration at day t by the concentration at day 1 for both POC and PON. The POC and PON concentrations were corrected by the C- and N-content of the attached prokaryotes (see [Section 2.3](#)). The vertical lines in the graph show the substitution time for the two pools of organic matter for each experiment ([Table 3](#)). Replicates ($n = 3$) were performed at days 1, 5, 10, 15, 22, and 30 and were used to feed our degradation model ([Section 2.5](#)).

3.2. Initial particulate carbohydrate composition (PCHO)

Similar to the POC, the initial concentrations of the PCHO-C in the 'N-stress' and 'Si-stress' cells on a per volume basis were approximately two and four times higher than those in the 'Nutrient-replete' cells (0.22, 0.40, and 0.11 pmol cell⁻¹, respectively). Note that the PCHO analyses do not discriminate between the PCHO arising from diatoms and those from prokaryotes.

Similar to the POC levels, the PCHO-C concentrations also peaked at day 1 and increased by 3.7%, 2.4%, and 1.1% of their initial concentrations in the 'Nutrient-replete', 'N-stress' and 'Si-stress' batches, respectively. Therefore, as observed with the POC degradation, the PCHO-C degradation rate constants were calculated from day 1. The monosaccharide composition at day 1 was dominated by ribose, galactose, and glucose in all of the batches, which accounted for more than 60 mol% of the total PCHO pool ([Table 2](#)).

The 'Nutrient-replete' batch was characterized by a higher ribose contribution (22 mol%) compared with the 'N-stress' and 'Si-stress' batches (4 and 11 mol%, respectively) at day 0, whereas the contribution of galactose varied only slightly between the three batches (29 to 38 mol%; [Table 2](#)). The contribution of glucose was significantly higher in the 'N-stress' batch compared with the 'Nutrient-replete' batch (Kruskal–Wallis test, $n = 9$, $p < 0.05$). The ribose concentrations and yields (Rib.-C/PCHO-C%) rapidly decreased over time in all of the experiments, indicating a selective extraction of this monosaccharide from the PCHO pool ([Table 2](#)). Interestingly, the 'Nutrient-replete' batch was particularly enriched in galacturonic acid (~8 mol%) compared with the 'N-stress', and 'Si-stress' batches (<2 mol%; [Table 2](#)). Finally, none of the other monosaccharides showed significant initial differences (at day 1) among the 'Nutrient-replete', 'N-stress', and 'Si-stress' batches.

3.3. Organic matter degradation

3.3.1. Bulk parameters (POC and PON)

As indicated above, an increase in the POC concentrations (approximately 7–30% of the initial POC) was observed at day 1 in the three batches. Therefore, the biotic degradation kinetics were calculated beginning at day 1. The POC degradation followed similar patterns in the three batches, with a first period of degradation in which the POC degraded faster followed by a second period of degradation in which the POC was degraded more slowly ([Fig. 3a](#)). The degradation rate constants of the first period were similar in the three batches ($0.11 \pm 0.03 \text{ d}^{-1}$, $0.096 \pm 0.002 \text{ d}^{-1}$, and $0.11 \pm 0.01 \text{ d}^{-1}$; [Table 3](#)); however, this was not the case for the substitution time, which was different among the three batches ($t_s = 5.9 \pm 0.6 \text{ d}$, $11.1 \pm 0.2 \text{ d}$ and $8.5 \pm 0.2 \text{ d}$).

At the end of the rapid degradation period, ~40% of the POC from the 'Nutrient-replete' diatoms was degraded, whereas this amount was ~60% for the N- and Si-stressed TW during the same period. During the second period, the POC was degraded at a significantly slower rate, with degradation rate constants of $0.040 \pm 0.001 \text{ d}^{-1}$, $0.018 \pm 0.001 \text{ d}^{-1}$, and $0.014 \pm 0.001 \text{ d}^{-1}$ for the 'Nutrient-replete', 'N-stress', and 'Si-stress' batches, respectively. Interestingly, the POC concentrations reached a "plateau" after 25 days of degradation and accounted for 27% of the initial POC in all three of the batches ([Fig. 3a](#)).

The degradation rate constants of the PON were consistently higher in the 'Nutrient-replete' batch for both of the pools (k_1 and k_2) than in the 'N- and Si-stress' batches ([Table 3](#); [Fig. 3b](#)). The degradation rate constants of the PON measured in the 'N- and Si-stress' batches only differed for the k_1 constant rates ([Table 3](#)). The second pool of the PON degraded with a similar degradation rate constant in the 'N- and Si-stress' batches ($k_2 \approx 0.020 \pm 0.001 \text{ d}^{-1}$). The t_s value was one half the value in the 'Nutrient-replete' batch ($5.0 \pm 0.6 \text{ d}$) compared with the 'N- and Si-stress' batches (~10.0 ± 0.6 d). Therefore, at the end of the biodegradation experiment (30 days), only 18% of the initial PON

Table 2
Elemental carbohydrate compositions (percentage of the total sugar, mol%) and the total PCHO-C concentrations (in μM) during the 30 days of the degradation. The PCHO yields are given as the percentage of total PCHO-C to the POC. Abbreviations: Fuc.—Fucose; Rha.—Rhamnose; Ara.—Arabinose; GlcN.—Glucosamine; Gal.—Galactose; Glc.—Glucose; Man.—Mannose; Xyl.—Xylose; Rib.—Ribose; GalUA.—Galacturonic Acid. The values given at days 1 and 30 are the mean of three measurements (see Fig. 3).

Experiment	Time (d)	Fuc.	Rha.	Ara.	GlcN.	Gal.	Glc.	Man.	Xyl.	Rib.	GalUA	PCHO-C	PCHO-C/POC
Nutrient-replete	0	2.73	8.10	0.32	1.03	37.53	5.51	5.53	9.34	21.97	7.95	30.01	2.03
	1	2.57	8.04	0.19	3.62	15.04	8.36	4.27	6.47	46.69	4.75	102.55	5.22
	6	4.78	15.19	1.02	4.99	15.37	9.55	9.95	13.29	16.97	8.89	85.99	8.06
	12	6.80	14.26	3.37	4.83	13.28	8.86	9.16	11.97	16.04	11.42	41.90	6.59
	25	7.07	13.59	1.86	7.06	13.11	11.78	9.49	15.72	7.21	13.11	36.74	7.66
	30	8.28	12.69	2.33	6.74	12.53	13.47	8.35	16.79	6.71	12.10	30.64	6.26
N-stress	0	5.37	7.98	0.29	1.30	28.59	32.43	6.29	13.04	3.54	1.18	77.77	1.75
	1	2.45	6.36	0.32	1.81	11.82	43.02	3.65	7.33	22.87	0.37	193.95	4.02
	6	4.16	10.91	0.36	3.52	12.76	28.53	7.57	10.52	20.13	1.56	164.45	4.97
	12	5.29	12.76	1.11	4.89	14.40	22.28	10.22	14.12	12.74	2.20	145.90	7.94
	18	5.56	12.50	1.18	5.04	15.09	24.50	10.83	13.29	9.34	2.67	108.54	6.39
	25	5.21	7.74	0.28	1.26	27.74	31.47	6.10	12.66	3.43	4.12	94.25	6.90
30	7.67	11.17	2.20	4.81	13.54	25.40	9.08	14.27	9.85	2.00	60.65	4.26	
Si-stress	0	4.10	11.38	0.30	2.01	37.62	5.20	8.13	18.65	10.56	2.04	114.93	3.05
	1	3.38	11.61	0.22	4.12	17.66	12.14	4.77	11.64	34.06	0.40	162.92	3.84
	6	3.23	12.11	0.23	5.13	8.14	19.72	5.00	9.67	36.77	0.00	219.95	6.78
	12	6.27	16.57	1.24	5.93	10.97	13.80	9.91	16.98	18.33	0.00	87.36	5.23
	18	7.15	16.22	1.57	7.41	11.89	13.53	11.82	17.91	12.50	0.00	57.51	3.54
	30	7.26	16.26	3.06	7.17	11.66	15.83	10.85	18.68	9.23	0.00	68.06	5.18

remained in the 'Nutrient-replete' batch, whereas 40% and 55% remained in the 'Si-stress' and the 'N-stress' batches, respectively.

3.3.2. Particulate carbohydrates (PCHO)

The degradation rate constants for the total PCHO-C were slightly lower but not significantly different in the 'N-stress' and 'Si-stress' batches ($0.04 \pm 0.01 \text{ d}^{-1}$) than in the 'Nutrient-replete' batch ($0.05 \pm 0.01 \text{ d}^{-1}$; Table 3; Fig. 4). At the end of the 30 days of degradation, 26% of the total PCHO-C remained in the 'Nutrient-replete' batch, whereas PCHO-C represented ~35% in the 'N-stress' and 'Si-stress' batches.

The degradation rate constants of the individual monosaccharides showed important differences in their decay (Table 3). Ribose was the monosaccharide with the highest degradation rate constants ($k = 0.073\text{--}0.215 \text{ d}^{-1}$) followed by glucose ($k = 0.028\text{--}0.071 \text{ d}^{-1}$), and galactose ($k = 0.018\text{--}0.060 \text{ d}^{-1}$). A slight, non-significant decrease in the galactose concentrations was observed in the 'N-stress' batch, with a degradation rate constant three times lower than that

of the 'Nutrient-replete' and 'Si-stress' batches ($k = 0.02 \pm 0.01 \text{ d}^{-1}$ versus $0.05 \pm 0.01 \text{ d}^{-1}$ and $0.06 \pm 0.02 \text{ d}^{-1}$, respectively, Fig. 5a). Similarly, the ribose degradation rate constants in the 'Nutrient-replete' and 'N-stress' batches were very different and three-times lower in the latter ($k = 0.21 \pm 0.05 \text{ d}^{-1}$ and $0.073 \pm 0.007 \text{ d}^{-1}$ in the 'Nutrient-replete' and 'N-stress' batches, respectively, Fig. 5b). The high variability of the ribose concentrations in the 'Si-stress' batch did not allow an accurate estimation of the kinetic parameters ($k = 0.07 \pm 0.04$, $p > 0.1$). This result was also the case for glucose, which showed a non-significant degradation rate constant very close to that measured in the 'Nutrient-replete' batch (Table 3; Fig. 5c). In the 'N-stress' batch, the glucose degradation rate constant was two times higher than that of the 'Nutrient-replete' batch ($k = 0.07 \pm 0.04 \text{ d}^{-1}$) indicating the presence of a labile pool of glucose-containing molecules.

The degradation rate constants of the other monosaccharides were variable, ranging from <0 (arabinose) to 0.027 d^{-1} (rhamnose). As a general trend, the degradation rate constants of these individual

Table 3
Estimated kinetic parameters for POC, PON, PCHO, and the individual monosaccharides (see equations in Section 2.5) during degradation of TW. The t_s value is the substitution time between the two pools of organic matter. The standard error (SE) is given for each estimation. Significant estimations are underlined ($p < 0.05$).

Kinetic parameters	Nutrient-replete						N-stress						Si-stress					
	k_1		k_2		t_s		k_1		k_2		t_s		k_1		k_2		t_s	
	Value	SE	Value	SE	Value	SE	Value	SE	Value	SE	Value	SE	Value	SE	Value	SE	Value	SE
POC (n = 34)	0.111	0.031	0.04	0.001	5.908	0.561	0.096	0.002	0.018	0.001	11.14	0.181	0.113	0.005	0.014	0.001	8.544	0.237
PON (n = 34)	<u>0.191</u>	0.099	<u>0.054</u>	0.001	<u>4.989</u>	0.587	<u>0.044</u>	0.002	<u>0.021</u>	0.001	<u>10.54</u>	0.639	<u>0.078</u>	0.002	<u>0.019</u>	0.001	<u>10.07</u>	0.127
Kinetic parameters	k (n = 9)						k (n = 10)						k (n = 9)					
	Value			SE			Value			SE			Value			SE		
Fuc.	0.004			0.01			0.002			0.006			0.005			0.005		
Rha.	0.027			0.011			0.017			0.01			0.022			0.009		
Ara.	-0.014			0.019			-0.015			0.016			<u>-0.057</u>			0.009		
GlcN.	0.022			0.01			0.01			0.013			<u>0.014</u>			0.01		
Gal.	<u>0.054</u>			0.01			0.018			0.009			<u>0.06</u>			0.018		
Glc.	<u>0.028</u>			0.01			0.071			0.037			0.029			0.02		
Man.	0.021			0.013			0.009			0.012			0.004			0.007		
Xyl.	0.012			0.011			0.012			0.007			0.016			0.007		
Rib.	0.215			0.054			0.050			0.007			0.073			0.043		
GalUA	<u>0.009</u>			0.009			-0.01			0.019			-			-		
Total PCHO	<u>0.046</u>			0.01			<u>0.036</u>			0.009			<u>0.036</u>			0.014		

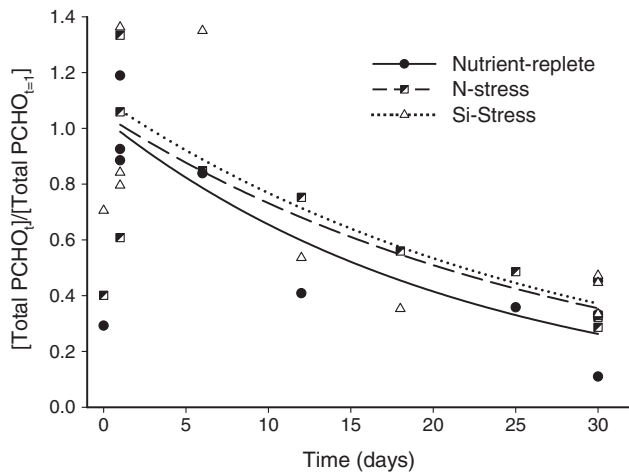


Fig. 4. Time course responses of the PCHO-C relative concentrations in the 'Nutrient-replete', 'N-stress', and 'Si-stress' batches. The relative concentrations were calculated by dividing the concentration at day t by the averaged concentration at day 1. The kinetics were estimated using Eq. (3) (Section 2.5). We used the concentration measured on day 1 as the initial concentration. All of the experimental points correspond to one measurement except at day 1 and day 30 ($n = 3$).

monosaccharides were higher in the 'Nutrient-replete' batch compared with the 'N and Si-stress' batches.

4. Discussion

4.1. Effect of N- and Si-starvation on the initial *T. weissflogii* composition

The effect of nutrient stress, including starvations, on the biochemical content (sugars, amino acids, and lipids) of diatoms has been addressed in previous studies for several diatom species (De La Rocha et al., 2010; Hou et al., 2007; Liu et al., 2012). These studies have shown dissimilarities in the physiological responses of the diatom, indicating a specific response against nutrient stress (Palmucci et al., 2011; Richardson and Cullen, 1995; Shifrin and Chisholm, 1981; Waite et al., 1992) and are in agreement with the present study. Our results showed that nitrogen and silicon starvations induced an increase in the carbon content per cell in TW (Table 1). Other studies have reported a decrease in the N content per cell during N starvation, whereas no changes have been observed during Si starvation (De la Rocha et al., 2010). Our results showed that the N content per cell also decreased during N-starvation and slightly increased during Si-starvation (Table 1) indicating that N- and/or Si-starvations have different effects on the carbon and nitrogen content of TW.

The carbohydrate (PCHO) concentrations in the 'Nutrient-replete' cells were 2–3 times lower than those found in the 'N-stress' and 'Si-stress' cells (Table 2), suggesting an increase in the PCHO levels during starvations, which is in agreement with previous investigations performed in other diatoms species (*T. pseudonana*; Harrison et al., 1990). Other studies performed on TW employing similar nutrient starvation conditions have reported a decrease in the amino acid and lipid content (Klein Breteler et al., 2005; Martin-Jézéquel, 1992; Shifrin and Chisholm, 1981). These results suggest that nutrient starvation has different effects on the organic matter components of the diatoms (carbohydrates, lipids, and amino acids). Carbohydrates in diatoms are generally divided into cellular and extracellular polysaccharides (Myklestad, 1995). In diatoms, it is well known that the genus *Thalassiosira* releases low levels of extracellular polysaccharides, primarily composed of glucose (Urbani et al., 2005), compared with another genus, such as *Chaetoceros* (Myklestad, 1995). The amount of extracellular polysaccharides released under a nutrient stress accounts for approximately 3% of the total cellular carbohydrate in TW (Myklestad, 1995). Carbohydrates are molecules that are primarily composed of carbon atoms, and their release as extracellular

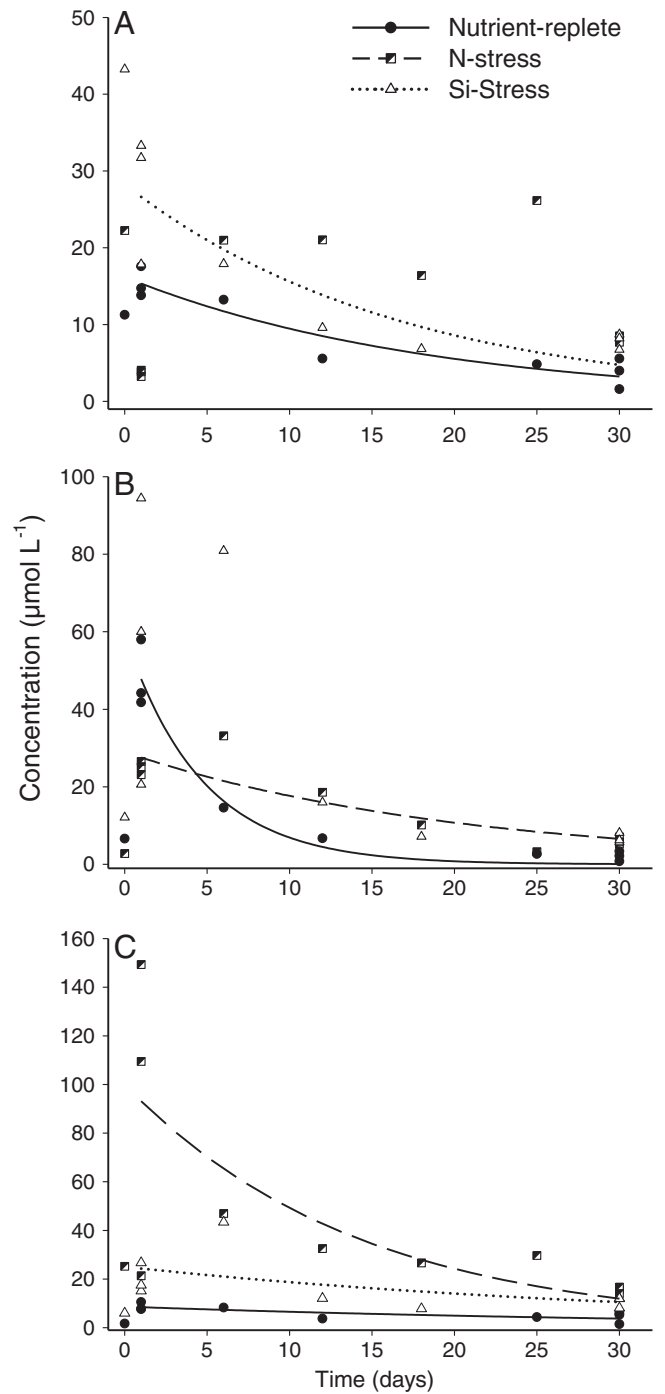


Fig. 5. Time course responses of (A) galactose, (B) ribose, and (C) glucose in the 'Nutrient-replete', 'N-stress', and 'Si-stress' batches. The kinetics were estimated using Eq. (3) (Section 2.5) and the concentrations at day 1 as the initial concentrations. The degradation rates for galactose (N-stress batch), ribose (Si-stress batch), and glucose (Si-stress batch) were no significant at the 0.05 level (see Table 3). All of the experimental points correspond to one measurement except at day 1 and day 30 ($n = 3$).

polysaccharides (EPS) during stress conditions may decrease the C/N ratio of the diatom cells to their 'initial' value (C/N value of = 5–7).

The changes in the carbohydrate concentration during stress conditions were also reflected in their individual sugar monomers, which have never been thoroughly examined in previous studies (Table 2). The relative abundance of most of the monosaccharides increased during Si-starvation (except for ribose and galacturonic acid), whereas the primary differences for the N-starvation experiment were observed in the relative abundances of glucose, ribose, and xylose. N-starvation

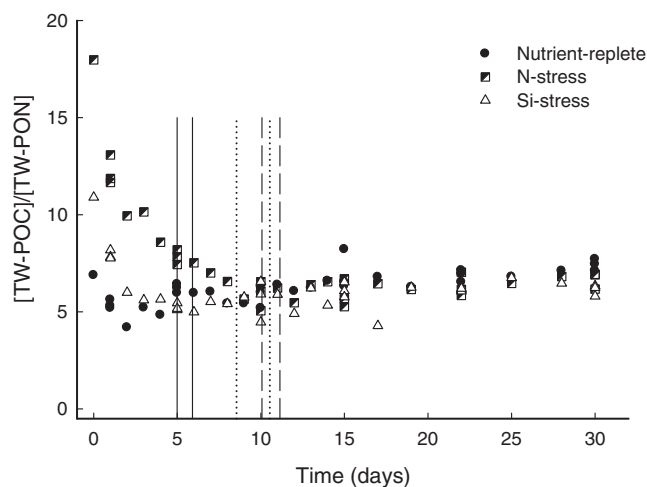


Fig. 6. Time course responses of the POC/PON ratio in the 'Nutrient-replete', 'N-stress', and 'Si-stress' batches during the TW biodegradation. As in Fig. 2, the vertical lines show the substitution t_s time (see Section 2.5) for the POC (bold) and PON (not bold) parameters.

strongly affected the glucose content of the cells (Table 2). Therefore, the high increase in the glucose relative abundance may suggest a preferential synthesis of glucose-rich polymers such as laminarin which are well known to be storage molecules in diatoms (Chiovitti et al., 2003; Størseth et al., 2005). The high relative abundance of ribose in the 'Nutrient-replete' cells most likely reflects the better physiological status of these cells because ribose-containing molecules (e.g., ATP and RNA) are involved in energy metabolism. Other studies have shown a decrease in the RNA synthesis in the 'N-stress' diatoms, implying a decrease in the ribose content of the cells, which is in agreement with our results (Hockin et al., 2012; Mock et al., 2008). High amounts of ribose in marine particulate organic matter is generally attributed to fresh material (Panagiotopoulos and Sempéré, 2005a, 2007), but it can also imply a good physiological status of the 'diatom' cells in the investigated sampling area.

The above results clearly suggest that Si-starvation may have a more pronounced effect on the cell's physiological status than on its metabolism functions. This result may indicate that silica-stress cells have lower energy requirements (no synthesis of glucose polymers) than nitrogen-stress cells. This result is in agreement with previous results on *T. pseudonana*, suggesting an uncoupling of Si with C metabolism (Claquin et al., 2002).

4.2. Effect of N- and Si-starvation on *T. weissflogii* organic matter degradation

As indicated above, the kinetic calculations of the POC and PON degradation suggested the presence of two pools of organic matter with different degradation rate constants (Table 3). These results suggest that both of these pools are composed of relatively biodegradable molecules, and certain of these molecules are most likely produced during starvation (extracellular sugars; Table 3 and Fig. 3a). Our results also showed that although the first order degradation rate constants (k_1) of the 'nutrient-replete', 'N-stress', and 'Si-stress' for the TW-POC were nearly similar during degradation, they corresponded to different substitution t_s values. The higher t_s values were observed during the nutrient stressed TW-POC degradation (t_s values of 8.5–11.4 days) compared with the "Nutrient replete" cells (t_s value of 5.9 days; Table 3). These results clearly indicate that the TW-intracellular molecules that constitute the labile TW-POC (first order rate constants) are degraded over a longer period in which the TW cells are submitted to "stress" conditions. This result may be partially explained by the increase in the carbon content of the TW cells in which labile compounds, such as carbohydrates, are produced during stress-conditions; therefore, additional time for their

degradation is required (Table 2). The degradation rate constants of the second pool (k_2) during the TW-POC degradation were nearly similar for the "stress-cells" but significantly lower than those of the "Nutrient-replete" cells ($k_{Si-stress} \sim k_{N-stress} \ll k_{nut-rep.}$; Table 3). These results indicate that the stress-conditions may increase the residence time (k^{-1}) of less labile organic molecules, which may affect their bioavailability in the environment.

In contrast to the POC, the first order degradation rate constants (k_1) of PON were clearly different between each batch (Table 3, Fig. 3b). Our results indicated that TW-PON appeared to become less labile after the N- and Si-starvations. These differences were reflected in the amount of diatom PON remaining at the end of each experiment (17.4%, 34.7% and 51.1% of the initial diatom PON in the 'Nutrient-replete', 'Si-stress', and 'N-stress' batches, respectively). These results may suggest a N-utilization from the TW intracellular N-compounds (proteins, nucleic acids, and/or ATP), which are well known to be very labile (Hockin et al., 2012). This result concurs with the low initial concentrations of ribose recorded in the "N- and Si-stress" TW-cells (Table 3), indicating that the ATP molecules (ribose and N-nucleobases-rich) are most likely the first to be exhausted at the beginning of the N-starvation.

Although the POC/PON ratios were high at the beginning of the degradation for the 'N- and Si-stress' cells, they reached values close to the Redfield C/N ratio after ~5–11 days of degradation (Fig. 6; Sarthou et al., 2005). This result suggests a preferential prokaryotic degradation of excess C-containing compounds and may explain the high degradation rate constant of glucose (an N-free compound) obtained in the 'N-stress'-experiment (most likely storage compounds) (Table 3; Fig. 5c). Interestingly, similar C/N ratios (6.1–6.7) have been obtained for sediment trap material collected from the Pacific Ocean (Hernes et al., 1996). The authors have interpreted these low values as a non-selective degradation of OC versus ON. Alternatively, this result may be due to a preferential selectivity that coincidentally maintains the low C/N values. Our results agree with these features, indicating a non-coincident selective degradation of excess C- and N-containing molecules.

The degradation rate constants of the PCHO were consistently lower than the first order degradation rate constants of the POC ($k_1 = 0.096$ – 0.11 d^{-1} ; Table 3) but higher than the second order degradation rate constants of the POC ($k_2 = 0.018$ – 0.040 d^{-1}), indicating that carbohydrates are most likely the second most labile component in TW after amino acids. The PCHO degradation rate constants were higher than the individual monosaccharides, except for ribose, which exhibited the highest rates in all of the experiments (Table 3). Therefore, it appears that the PCHO rate constants reflect an average of the different degradation rates corresponding to each monosaccharide, indicating differences in their initial macromolecular origin (e.g., storage vs structural carbohydrates).

For example, the galactose degradation rate constants were higher in the 'Nutrient-replete' and 'Si-stress' cell degradation experiments than in the 'N-stress' experiment (Table 3; Fig. 5a). This monosaccharide is primarily found in cell wall polysaccharides (Cowie and Hedges, 1996; Hecky et al., 1973), whereas it is also reported in excreted exopolymeric substances (Giroldo et al., 2003). Based on the ectoenzymatic bacterial activities in sediments, Arnosti (2000) has suggested that the former could be less labile than the latter. Based on the above literature observations and the higher degradation rate constants observed for the 'Nutrient-replete' and 'Si-stress' experiments (Table 3), we may hypothesize that galactose would primarily originate from the excretion of the EPS (in the case of the 'Nutrient-replete' and 'Si-stress' experiments), which are known to be stimulated during nutrient deficiency. Alternatively, galactose may also originate from the cell wall polysaccharides in the 'N-stress' cell experiment based on its low degradation constant.

The ribose degradation rate constants showed important differences among the starvation experiments. The high degradation rate constant

recorded for the 'Nutrient-replete' experiment reflects the good physiological status of the TW cells and agrees with the elevated ribose concentrations measured at T_0 (Table 3, Fig. 5b). This high rate most likely illustrates the hydrolysis of ATP polymers (rich in ribose), whereas the low rates measured in N- and Si-stress cells most likely indicate the exhaustion of the ATP molecules at the beginning of the N-starvation (see above). This result is further supported by the similarity of the first order decay constants of the PON and those of ribose for all of the biodegradation experiments (Table 3).

Similarly, the degradation rate constants measured for glucose may provide indications about the nature of the original polymer. Glucose may originate from laminarin (Størseth et al., 2005) or callose (Tesson and Hildebrand, 2013), which are sugar-polymers involved in energy storage (laminarin) or fibrillar structure (callose). The high degradation rate constant (indicating increased bioavailability) obtained for the glucose in the 'N-stress' TW most likely suggests that glucose may originate from laminarin (Table 3; Fig. 5c).

Our results also showed that the concentrations of some of the monosaccharides showed a small increase after day 1. This was especially the case for arabinose, galacturonic acid, and mannose (Table 2). This result may be related to the increase of the prokaryotic concentration which peaked at day 3 (Fig. 2), most likely suggesting that these monosaccharides may be *de novo* produced by prokaryotes. However, the prokaryotic carbon represented a small percentage of this increase (see above) and cannot solely explain the increase in the concentrations of these sugars.

The increase in the mannose and arabinose concentrations in 'Si-stress' batch may be related to other factors, such as a release of polysaccharides from the frustule of TW, which is dissolved slowly over time. Earlier studies on four different diatom species indicated that the polysaccharides released after the dissolution of the frustules are primarily composed of a mannose backbone bearing uronic acid residues (Chiovitti et al., 2005). In our study, the degradation rate constant of galacturonic acid in the 'Si-stress' batch was completely different from that of the two other batches (Table 3). This result may be explained by a modified frustule structure affected by the Si starvation (Moriceau et al., 2007; Soler, 2010). This finding strongly agrees with the high correlation between the mannose and galacturonic acid concentrations over time in the 'Nutrient-replete' batch ($r = 0.88$).

4.3. Biogeochemical implications on the vertical transport of the nutrient-stressed TW cells

In a marine environment, diatoms are often subjected to nutrient depletion depending on the environmental conditions. Although it has been suggested that diatoms may regulate their buoyancy to sink into a deeper nutrient-rich layer of the euphotic zone, the effect of the nutrient stress on their morphology is not well known (Kemp et al., 2006 and references therein). The *Thalassiosira* species, in particular, have been suggested to be very nutrient-sensitive, which significantly affects their sinking rate (Waite et al., 1992). Other studies have demonstrated that nutrient-stressed TW cells increase their carbohydrate content, resulting in an increase in their density and their aggregation; therefore, they sink rapidly in the water column (Richardson and Cullen, 1995). Our results also showed an increase in the carbohydrate content of the TW cells under N- and Si-depleted conditions, which may potentially impact the behavior of TW cells (changes in sinking rates, aggregation etc.) in the natural environment. Furthermore, the degradation rate constants (k_1 , and k_2) of the nutrient limited cells generally decreased compared with the nutrient-replete cells (Table 3), which further may imply a potentially higher amount of carbon for export under nutrient-stress conditions.

On the other hand, other studies indicated that the decrease in the cell size due to the nutrient-limitation may attenuate the sinking rates because of the dissolution of silicon, which forms the cell frustule,

resulting in lighter TW cells (Boutorh, 2014; De la Rocha and Passow, 2007). Our experiments also showed a decrease in the bSiO₂ content in the stressed TW cells (Table 1). Overall, these results highlight the complexity of evaluating the relationship between the environmental factors (nutrient-limitation) and the sinking velocity of diatom frustules. These factors clearly influence the sequestration of organic carbon in the deep ocean at the spatial (differences in species composition) and temporal (differences in physiological status) scales and clearly have an important effect on the microbial carbon pump.

5. Summary and concluding remarks

This study explored the degradation features of the TW cells grown under nutrient-stress conditions (N- and Si-limitations), similar to those occurring in a natural environment. Our results showed that the TW stressed-cells increased their carbon content (approximately two times) and their C/N ratios (2–3 times) compared with the 'Nutrient-replete' cells (Table 1; Fig. 6). This carbon increase was accompanied by a decrease in the bSiO₂ in the nutrient-stressed cells, indicating a structural modification of the TW frustule. From a chemical composition view point, this increase in the carbon was essentially reflected in the carbohydrate component of the TW cells. Hence, the carbohydrate (PCHO) concentrations in the 'Nutrient-replete' cells were 2–3 times lower than those found in the 'N-stress' and 'Si-stress' cells (Table 2) suggesting an increase in the PCHO content during starvation. The 'N-stress' and 'Si-stress' cells were characterized by higher amounts of glucose (5–32 mol%) and xylose (13–19 mol%) compared with the 'Nutrient-replete' cells, which were dominated by ribose (22 mol%), indicating differences in the physiological status of the TW cells and/or the synthesis of storage/structural polysaccharides under different nutrient growth conditions.

The biodegradation experiments of the 'Nutrient-replete', 'N-stress', and 'Si-stress' TW cells showed that the first order degradation rate constants for the POC were similar ($k_1 = 0.096$ – 0.113 d⁻¹) but were characterized by different substitution times, indicating that intracellular and labile TW compounds require longer times to be degraded under stress conditions (Table 3). The second order degradation rate constants (k_2) of the POC were approximately two times higher for the 'Nutrient-replete' cells than the 'N-stress' and 'Si-stress' cells, indicating that nutrient limited conditions may increase the residence time (k^{-1}) of less labile intracellular TW compounds. The PCHO degradation rates were between the first and the second order degradation rates of the POC, suggesting that the carbohydrates are most likely the second most labile component of TW after the amino acids.

Ribose, glucose, and galactose exhibited the highest degradation rate constants in the various experiments which further reflects the differences in their initial macromolecular origin due to different C and N allocation (e.g., storage vs structural carbohydrates) under nutrient-limited conditions and highlights the changes in the organic matter quality during degradation.

Acknowledgments

We thank D. Delmas for the prokaryote counting during the degradation experiment and C. Labry for the seawater sampling at the Brest Somlit station. We also thank A. Masson for the POC/PON measurements as well as the two anonymous reviewers for their constructive comments. This study was supported by the UTIL (LEFE/CYBER, CNRS/INSU) and MANDARINE (grant No 2008-10372) (Région Provence Alpes Côte d'Azur) projects. M. Suroy was supported by a Ph.D grant from Aix-Marseille University [SS].

References

Arnosti, C., 2000. Substrate specificity in polysaccharide hydrolysis: contrasts between bottom water and sediments. *Limnol. Oceanogr.* 45, 1112–1119.

- Aumont, O., Maier-Reimer, E., Blain, S., Monfray, P., 2003. An ecosystem model of the global ocean including Fe, Si, P colimitations. *Glob. Biogeochem. Cycles* 17, 1–26.
- Bidle, K.D., Manganello, M., Azam, F., 2002. Regulation of oceanic silicon and carbon preservation by temperature control on bacteria. *Science* 298, 1980–1984.
- Boutorh, J., 2014. Impact des conditions nutritionnelles sur la dissolution de la silice biogénique des diatomées à travers l'étude de la variabilité de la structure biphasique du frustule. Ph.D. Thesis. Université de Bretagne occidentale, France, p. 181.
- Brown, M.R., Jeffrey, S.W., Volkman, J.K., Dunstan, G.A., 1997. Nutritional properties of microalgae for mariculture. *Aquaculture* 151, 315–331.
- Brzezinski, M.A., 1985. The Si:C:N ratio of marine diatoms: interspecific variability and the effect of some environmental variables. *J. Phycol.* 21, 347–357.
- Buesseler, K.O., 1998. The decoupling of production and particulate export in the surface ocean. *Glob. Biogeochem. Cycles* 12, 297–310.
- Chiovitti, A., Higgins, M.J., Harper, R.E., Wetherbee, R., 2003. The complex polysaccharides of the raphid diatom *Pinnularia viridis* (Bacillariophyceae). *J. Phycol.* 39, 543–554.
- Chiovitti, A., Harper, R.E., Willis, A., Bacic, A., Mulvaney, P., Wetherbee, R., 2005. Variations in the substituted 3-linked mannans closely associated with the silicified walls of diatoms. *J. Phycol.* 41, 1154–1161.
- Claquin, P., Martin-Jézéquel, V., Kromkamp, J.C., Veldhuis, M., Kraay, G., 2002. Uncoupling of silicon compared with carbon and nitrogen metabolisms and the role of the cell cycle in continuous cultures of *Thalassiosira pseudonana* (Bacillariophyceae) under light, nitrogen, and phosphorus control. *J. Phycol.* 38, 922–930.
- Core Team, R., 2012. R: A Language and Environment for Statistical Computing. R Foundation for Statistical Computing, Vienna, Austria.
- Cowie, G.L., Hedges, J.L., 1984. Carbohydrate sources in a coastal marine environment. *Geochim. Cosmochim. Acta* 48, 2075–2087.
- Cowie, G.L., Hedges, J.L., 1996. Digestion and alteration of the biochemical constituents of a diatom (*Thalassiosira weissflogii*) ingested by an herbivorous zooplankton (*Calanus pacificus*). *Limnol. Oceanogr.* 41, 581–594.
- De La Rocha, C.L., Passow, U., 2007. Factors influencing the sinking of POC and the efficiency of the biological carbon pump. *Deep-Sea Res. II* 54, 639–658.
- De La Rocha, C.L., Terbrüggen, A., Völker, C., Hohn, S., 2010. Response to and recovery from nitrogen and silicon starvation in *Thalassiosira weissflogii*: growth rates, nutrient uptake and C and N content per cell. *Mar. Ecol. Prog. Ser.* 412, 57–68.
- Duhamel, S., Moutin, T., Van Wambeke, F., Van Mooy, B., Raimbault, P., Chaustra, H., 2007. Growth and specific P-uptake rates of bacterial and phytoplanktonic communities in the Southeast Pacific (BIOSPE cruise). *Biogeosciences* 4, 941–956.
- Engel, A., Abramson, L., Szlosek, J., Liu, Z., Stewart, G., Hirschberg, D., Lee, C., 2009. Investigating the effect of ballasting by CaCO₃ in *Emiliania huxleyi*, II: Decomposition of particulate organic matter. *Deep-Sea Res. II* 56, 1408–1419.
- Fagerbakke, K.M., Heldal, M., Norland, S., 1996. Content of carbon, nitrogen, oxygen, sulfur and phosphorus in native aquatic and cultured bacteria. *Aquat. Microb. Ecol.* 10, 15–27.
- Falkowski, P.G., 1997. Evolution of the nitrogen cycle and its influence on the biological sequestration of CO₂ in the ocean. *Nature* 246 (170–170).
- Giraudoux, P., 2012. pgirmess: Data analysis in ecology. R package version 1.5.4. <http://CRAN.R-project.org/package=pgirmess>.
- Giroldo, D., Vieira, A.A.H., Paulsen, B.S., 2003. Relative increase of deoxy sugars during microbial degradation of an extracellular polysaccharide released by a tropical freshwater *Thalassiosira* sp. (Bacillariophyceae). *J. Phycol.* 39, 1109–1115.
- Goutx, M., Wakeham, S.G., Lee, C., Duflos, M., Guigüe, C., Liu, Z., Moriceau, B., Sempéré, R., Tedetti, M., Xue, J., 2007. Composition and degradation of marine particles with different settling velocities in the northwestern Mediterranean Sea. *Limnol. Oceanogr.* 52, 1645–1664.
- Harrison, P.J., Thompson, P.A., Calderwood, G.S., 1990. Effects of nutrient and light limitation on the biochemical composition of phytoplankton. *J. Appl. Phycol.* 2, 45–56.
- Harvey, H.R., Macko, S.A., 1997. Kinetics of phytoplankton decay during simulated sedimentation: changes in lipids under oxic and anoxic conditions. *Org. Geochem.* 27, 129–140.
- Harvey, H.R., Tuttle, J.H., Tyler Bell, J., 1995. Kinetics of phytoplankton decay during simulated sedimentation: changes in biochemical composition and microbial activity under oxic and anoxic conditions. *Geochim. Cosmochim. Acta* 59, 3367–3377.
- Hecky, R.E., Mopper, K., Kilham, P., Degens, E.T., 1973. The amino acid and sugar composition of diatom cell-walls. *Mar. Biol.* 19, 323–331.
- Hernes, P.J., Hedges, J.L., Peterson, M.L., Wakeham, S.G., Lee, C., 1996. Neutral carbohydrate geochemistry of particulate material in the central equatorial Pacific. *Deep-Sea Res. II* 43, 1181–1204.
- Hildebrand, M., 2002. Lack of coupling between silicon and other elemental metabolisms in diatoms. *J. Phycol.* 38, 841–843.
- Hockin, N.L., Mock, T., Mulholland, F., Kopriva, S., Malin, G., 2012. The response of diatom central carbon metabolism to nitrogen starvation is different from that of green algae and higher plants. *Plant Physiol.* 158, 299–312.
- Honda, M.C., Watanabe, S., 2010. Importance of biogenic opal as ballast of particulate organic carbon (POC) transport and existence of mineral ballast-associated and residual POC in the Western Pacific Subarctic Gyre. *Geophys. Res. Lett.* 37, L02605. <http://dx.doi.org/10.1029/2009GL01521>.
- Hou, J.J., Huang, B.Q., Cao, Z.R., 2007. Effects of nutrient limitation on pigments in *Thalassiosira weissflogii* and *Prorocentrum donghaiense*. *J. Integr. Plant Biol.* 49, 686–697.
- Iversen, M.H., Ploug, H., 2013. Temperature effects on carbon-specific respiration rate and sinking velocity of diatom aggregates—potential implications for deep ocean export processes. *Biogeosciences* 10, 4073–4085.
- Kemp, A.E.S., Pearce, R.B., Grigorov, I., Rance, J., Lange, C.B., Quilty, P., Salter, I., 2006. Production of giant marine diatoms and their export at oceanic frontal zones: implications for Si and C flux from stratified oceans. *Glob. Biogeochem. Cycles* 20, GB4S04. <http://dx.doi.org/10.1029/2006GB002698>.
- Klein Breteler, W.C.M., Schogt, N., Rampen, S.W., 2005. Effect of diatom nutrient limitation on copepod development: the role of essential lipids. *Mar. Ecol. Prog. Ser.* 291, 125–133.
- Lahaman, F., Jusoh, A., Ali, N., Lam, A.S., Endut, A., 2013. Effect of conway medium on the growth of six genera of South China Sea marine microalgae. *Bioresour. Technol.* 141, 75–82.
- Legendre, L., Rivkin, R.B., 2002. Fluxes of carbon in the upper ocean: regulation by food-web control nodes. *Mar. Ecol. Prog. Ser.* 242, 95–109.
- Liu, W., Huang, Z., Li, P., Xia, J., Chen, B., 2012. Formation of triacylglycerol in *Nitzschia closterium* f. minutissima under nitrogen limitation and possible physiological and biochemical mechanisms. *J. Exp. Mar. Biol. Ecol.* 418–419, 24–29.
- Logan, B.E., Passow, U., Alldredge, A.L., Grossart, H.-P., Simon, M., 1995. Rapid formation and sedimentation of large aggregates is predictable from coagulation rates (half-lives) of transparent exopolymer particles (TEP). *Deep-Sea Res. II* 42, 203–214.
- Lynn, S.G., Kilham, S.S., Kreeger, D.A., Interlandi, S.J., 2000. Effect of nutrient availability on the biochemical and elemental stoichiometry in the freshwater diatom *Stephanodiscus minutulus* (Bacillariophyceae). *J. Phycol.* 36, 510–522.
- Martin, P., Lampitt, R.S., Jane Perry, M., Sanders, R., Lee, C., D'Asaro, E., 2011. Export and mesopelagic particle flux during a North Atlantic spring diatom bloom. *Deep-Sea Res. I* 58, 338–349.
- Martin-Jézéquel, V., 1992. Effect of Si-status on diel variation of intracellular free amino acids in *Thalassiosira weissflogii* under low-light intensity. *Hydrobiologia* 238, 159–167.
- Martin-Jézéquel, V., Hildebrand, M., Brzezinski, M.A., 2000. Silicon metabolism in diatoms: implications for growth. *J. Phycol.* 36, 821–840.
- Mock, T., Samanta, M.P., Iversen, V., Berthiaume, C., Robison, M., Holtermann, K., Durkin, C., Bondurant, S.S., Richmond, K., Rodesch, M., Kallas, T., Huttlin, E.L., Cerrina, F., Sussman, M.R., Armbrust, E.V., 2008. Whole-genome expression profiling of the marine diatom *Thalassiosira pseudonana* identifies genes involved in silicon bioprocesses. *Proc. Natl. Acad. Sci. U. S. A.* 105, 1579–1584.
- Moore, J.K., Doney, S.C., Glover, D.M., Fung, I.Y., 2002. Iron cycling and nutrient-limitation patterns in surface waters of the World Ocean. *Deep-Sea Res. II* 49, 463–507.
- Moriceau, B., Garvey, M., Ragueneau, O., Passow, U., 2007. Evidence for reduced biogenic silica dissolution rates in diatom aggregates. *Mar. Ecol. Prog. Ser.* 333, 129–142.
- Moriceau, B., Goutx, M., Guigüe, C., Lee, C., Armstrong, R.A., Duflos, M., Tamburini, C., Charrière, B., Ragueneau, O., 2009. Si–C interactions during degradation of the diatom *Skeletonema marinoi*. *Deep-Sea Res. II* 56, 1381–1395.
- Myklesstad, S.M., 1995. Release of extracellular products by phytoplankton with special emphasis on polysaccharides. *Sci. Total Environ.* 165, 155–164.
- Nelson, D.M., Tréguer, P., Brzezinski, M.A., Leynaert, A., Quéguiner, B., 1995. Production and dissolution of biogenic silica in the ocean: revised global estimates, comparison with regional data and relationship to biogenic sedimentation. *Glob. Biogeochem. Cycles* 9, 359–372.
- Nieuwenhuize, J., Maas, Y.E.M., Middelburg, J.J., 1994. Rapid analysis of organic carbon and nitrogen in particulate materials. *Mar. Chem.* 45, 217–224.
- Palmucci, M., Ratti, S., Giordano, M., 2011. Ecological and evolutionary implications of carbon allocation in marine phytoplankton as a function of nitrogen availability: a Fourier transform infrared spectroscopy approach. *J. Phycol.* 47, 313–323.
- Panagiotopoulos, C., Sempéré, R., 2005a. The molecular distribution of combined aldoses in sinking particles in various oceanic conditions. *Mar. Chem.* 95, 31–49.
- Panagiotopoulos, C., Sempéré, R., 2005b. Analytical methods for the determination of sugars in marine samples: a historical perspective and future directions. *Limnol. Oceanogr.* 3, 419–454.
- Panagiotopoulos, C., Sempéré, R., 2007. Sugar dynamics in large particles during in vitro incubation experiments. *Mar. Ecol. Prog. Ser.* 330, 67–74.
- Panagiotopoulos, C., Wurl, O., 2009. Spectrophotometric and chromatographic analysis of carbohydrates in marine samples. In: Wurl, O. (Ed.), *Practical Guidelines for the Analysis of Seawater*. Taylor and Francis, pp. 49–65.
- Panagiotopoulos, C., Sempéré, R., Obernosterer, I., Striby, L., Goutx, M., Van Wambeke, F., Gautier, S., Lafont, R., 2002. Bacterial degradation of large particles in the southern Indian Ocean using in vitro incubation experiments. *Org. Geochem.* 33, 985–1000.
- Panagiotopoulos, C., Sempéré, R., Para, J., Raimbault, P., Rabouille, C., Charrière, B., 2012. The composition and flux of particulate and dissolved carbohydrates from the Rhone River into the Mediterranean Sea. *Biogeosciences* 9, 1827–1844.
- Richardson, T.L., Cullen, J.J., 1995. Changes in buoyancy and chemical composition during growth of a coastal marine diatom: ecological and biogeochemical consequences. *Mar. Ecol. Prog. Ser.* 128, 77–90.
- Sarthou, G., Timmermans, K.R., Blain, S., Tréguer, P., 2005. Growth physiology and fate of diatoms in the ocean: a review. *J. Sea Res.* 53, 25–42.
- Shifrin, N.S., Chisholm, S.W., 1981. Phytoplankton lipids interspecific differences and effects of nitrate, silicate and light-dark cycles. *J. Phycol.* 17, 374–384.
- Smetacek, V., 1985. Role of sinking in diatom life-history cycles: ecological, evolutionary and geological significance. *Mar. Biol.* 84, 239–251.
- Soler, C., 2010. Impact des conditions de croissance sur le métabolisme et les interactions Si-OC des diatomées—conséquences sur la vitesse de reminéralisation de la silice biogène et de la matière organique. Ph.D. Thesis. Université de Bretagne Occidentale, France, p. 207.
- Sorhannus, U., Ortíz, J.D., Wolf, M., Fox, M.G., 2010. Microevolution and speciation in *Thalassiosira weissflogii* (Bacillariophyta). *Protist* 161, 237–249.

- Størseth, T.R., Hansen, K., Reitan, K.I., Skjermo, J., 2005. Structural characterization of β -D-(1 \rightarrow 3)-glucans from different growth phases of the marine diatoms *Chaetoceros mülleri* and *Thalassiosira weissflogii*. *Carbohydr. Res.* 340, 1159–1164.
- Suroy, M., Boutorh, J., Moriceau, B., Goutx, M., 2014. Fatty acids associated to frustule of diatoms and their fate during degradation—a case study in *Thalassiosira weissflogii*. *Deep-Sea Res.* 1 86, 21–31.
- Tamburini, C., Garcin, J., Grégori, G., Leblanc, K., Rimmelin, P., Kirchman, D.L., 2006. Pressure effects on surface Mediterranean prokaryotes and biogenic silica dissolution during a diatom sinking experiment. *Aquat. Microb. Ecol.* 43, 267–276.
- Tesson, B., Hildebrand, M., 2013. Characterization and localization of insoluble organic matrices associated with diatom cell walls: insight into their roles during cell wall formation. *PLoS ONE* 8 (4), e61675. <http://dx.doi.org/10.1371/journal.pone.0061675>.
- Thornton, D.C.O., 2002. Diatom aggregation in the sea: mechanisms and ecological implications. *Eur. J. Phycol.* 37, 149–161.
- Turley, C.M., Mackie, P.J., 1994. Biogeochemical significance of attached and free-living bacteria and the flux of particles in the NE Atlantic Ocean. *Mar. Ecol. Prog. Ser.* 115, 191–203.
- Turner, J.T., 2002. Zooplankton fecal pellets, marine snow and sinking phytoplankton blooms. *Aquat. Microb. Ecol.* 27, 57–102.
- Uitz, J., Claustre, H., Gentili, B., Stramski, D., 2010. Phytoplankton class-specific primary production in the world's oceans: seasonal and interannual variability from satellite observations. *Global Biogeochem. Cycles* 24, GB3016. <http://dx.doi.org/10.1029/2009GB003680>.
- Urbani, R., Magaletti, E., Sist, P., Cicero, A.M., 2005. Extracellular carbohydrates released by the marine diatoms *Cylindrotheca closterium*, *Thalassiosira pseudonana* and *Skeletonema costatum*: effect of P-depletion and growth status. *Sci. Total Environ.* 353, 300–306.
- Velji, M.I., Albright, L.J., 1986. Microscopic enumeration of attached marine bacteria of seawater, marine sediment, fecal matter, and kelp blade samples following pyrophosphate and ultrasound treatments. *Can. J. Microbiol.* 32, 121–126.
- Volk, T., Hoffert, M.I., 1985. Ocean carbon pumps: analysis of relative strengths and efficiencies in ocean-driven atmospheric CO₂ changes. In: Sunquist, E.T., Broecker, W.S. (Eds.), *The Carbon Cycle and Atmospheric CO₂: Natural Variations Archean to Present*. American Geophysical Union, Washington, DC, pp. 99–110.
- Waite, A.M., Bienfang, P., Harrison, P.J., 1992. Spring bloom sedimentation in a sub-arctic ecosystem. I. Nutrient sensitivity. *Mar. Biol.* 114, 119–129.
- Walne, P.R., 1966. Experiments in the large scale culture of the larvae of *Ostrea edulis* L. *Fish. Investig. Series II XXV* (4) (52 pp.).